



PII S0016-7037(02)01040-2

Outer-sphere electron transfer kinetics of metal ion oxidation by molecular oxygen

KEVIN M. ROSSO^{1,*} and JAMES J. MORGAN²¹W. R. Wiley Environmental Molecular Sciences Laboratory, Pacific Northwest National Laboratory, P.O. Box 999, K8-96, Richland, WA 99352, USA²Department of Environmental Science and Engineering, California Institute of Technology, Pasadena, CA 91125, USA

(Received April 4, 2002; accepted in revised form July 3, 2002)

Abstract—Density functional theory molecular orbital calculations and Marcus theory have been combined to assess the rates and physicochemical factors controlling the outer-sphere oxidation of divalent V, Cr, Mn, Fe, and Co aquo and hydroxo ions by O₂ in homogeneous aqueous solution. Key quantities in the elementary oxidation step include the inner-sphere component of the reorganization energy, the thermodynamic driving force, and electrostatic work terms describing the interactions occurring, in this case, between the net charges on the product species. Collectively, these factors and their interplay have a large influence on the rate of the oxidation cross-reaction.

An inner-sphere pathway for the self-exchange reactions and oxidation by O₂ of Mn²⁺ and Cr²⁺ ions has been supported indirectly in this study by comparing predicted outer-sphere rates with the results of previous experiments. Likewise, an outer-sphere pathway is suggested for the similar sets of reactions involving the V, Fe, and Co ions. An assessment of the self-exchange reaction for the oxygen/superoxide couple has led to predicted rates in excellent agreement with direct measurements. Predicted rates of oxidation for the hexaquo Fe ion are also in agreement with experiment, while the predicted rates for the outer-sphere oxidation of its hydrolysis products are ~2 to 3 (monohydroxo) and ~4 (dihydroxo) orders of magnitude slower than the observed rates. This suggests an inner-sphere pathway is appropriate to explain the relatively fast rates observed for the hydrolyzed Fe species. Copyright © 2002 Elsevier Science Ltd

1. INTRODUCTION

The movement and bioavailability of redox-active metals such as iron, manganese, and chromium in natural waters can depend critically on their rates of reaction with dissolved molecular oxygen. In sea or lake environments, dissolved oxygen concentrations can change markedly and irregularly between the surface in contact with the atmosphere and the sediment layers on the bottom (Alldredge and Cohen, 1987; Stumm and Morgan, 1996). Steep redox gradients can also occur at the boundaries of polluted groundwater plumes (McGuire et al., 2000) and in acid mine drainage systems (Benner et al., 2000). The rate of transformation of metal ions as they traverse redox boundaries, where not catalyzed by biologic activity or mineral surfaces (e.g., Sung and Morgan, 1981; Emerson et al., 1982), is often controlled by the rate of reaction with oxygen. Because homogeneous electron transfer reactions with oxygen can be slow, redox equilibrium may never be reached in some settings (Keating and Bahr, 1998).

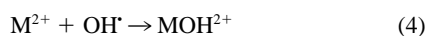
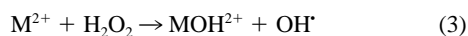
A primary example is the slow oxidation of Mn²⁺ by oxygen, where thermodynamics predicts that the most stable form of Mn is a solid-phase oxide (Bricker, 1965). This transformation has been shown to be kinetically inhibited for time periods on the scale of months (Giovanoli, 1980; Diem and Stumm, 1984). Predictive models based on thermodynamic redox equilibria aid in the analysis of such systems, as they can bracket the conditions toward which the system is proceeding. But their usefulness is typically limited by unknown kinetics. Information regarding the rates of individual electron transfer reactions

is therefore a prerequisite for understanding the speciation and cycling of metals in environments where disequilibrium dominates. These facts have formed the basis for numerous experimental studies intent on describing the homogeneous oxidation kinetics of metals such as Fe²⁺ (Singer and Stumm, 1970; Lowson, 1982; Millero, 1985, 1989; Millero et al., 1987; Millero and Izaguirre, 1989; King et al., 1995; King, 1998), Mn²⁺ (Hem, 1963; Morgan, 1967; Diem and Stumm, 1984), and Cr²⁺ (Sellers and Simic, 1976; Bakac and Espenson, 1993; Bakac et al., 1995). However, a large knowledge gap still exists regarding the molecular-scale processes underlying the rate behavior observed experimentally at macroscopic scales.

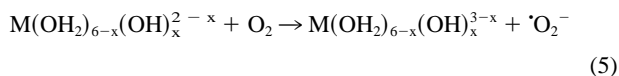
In this study, we employ molecular orbital calculations and Marcus theory to investigate the kinetics of and fundamental physiochemical controls on elementary electron transfer reactions between important redox-active metal aquo ions and molecular oxygen in solution. We examine the M^{2+/3+} oxidation reaction of the metal series V, Cr, Mn, Fe, and Co. This series was chosen because it includes typically important trace metals present in many natural waters (Stumm and Morgan, 1996) as well as the fact that as a set, they exhibit a wide range of oxidation rate behavior (Creutz and Sutin, 1986). The experimental literature database for these reactions is also extensive and provides rate constants for direct comparison with our theoretical rates.

The oxidation rate of these metals is generally found to be strongly pH dependent and first-order with respect to the metal ion (Stumm and Morgan, 1996). A number of oxidation mechanisms have been proposed to account for the observed rate behavior (Fallab, 1967). The most generally accepted step-wise oxidation scheme is the Haber-Weiss mechanism (Haber and Weiss, 1934):

* Author to whom correspondence should be addressed (kevin.rosso@pnl.gov).



whereby the first step involving electron transfer from the metal ion to the molecular oxygen molecule is rate-limiting and therefore is the reaction that controls the overall rate (Fallab, 1967). As this scheme has been useful in correctly describing most of the experimental rate data (Stumm and Morgan, 1996), we adopt a form of Eqn. 1 (protonation of the superoxide radical ignored) as the reaction of interest for the theoretical rate treatment in this investigation. It is likely that the most reactive form of the metal ion will be a hydrolyzed species (Stumm and Morgan, 1996). To explore the dependence of the electron transfer rate on metal ion speciation, we model the electron transfer rate for the hexaquo metal ion and its first two hydrolysis species as well. Thus, the set of elementary metal oxidation reactions we consider consists of all



where $\text{M} = \text{V}, \text{Cr}, \text{Mn}, \text{Fe}, \text{Co}$ and $x = 0 - 2$. Here we attempt to develop a better understanding of reactions of this type.

Very little is known about the structure of the encounter complex formed between the metal ions and the oxygen molecule. In this regard, electron transfer reactions can generally be subdivided into two types, those following an inner vs. outer-sphere mechanism. In the former, oxygen either interacts with the metal via a bridging ligand or by entering the coordination sphere of the metal ion through a ligand exchange process, and in the latter, oxygen interacts with the metal across discrete, intact coordination environments. In any particular reaction, the preference can be affected by solution parameters such as pH, because it can affect the lability of inner shell ligands (e.g., Nordin et al., 1998). Where ligand exchange is slower than electron transfer, an outer-sphere mechanism is usually assumed. Where ligand exchange is faster than electron transfer, either mechanism could be operative. In this case, an inner-sphere mechanism could be ascribed to a relatively fast electron transfer reaction because of the more intimate electronic interaction between the metal center and oxygen molecule, whereas the outer-sphere reaction represents a weaker electronic interaction. But there is a host of other factors that must be considered before this conclusion could be drawn, such as the relative rates of inner- vs. outer-sphere encounter complex formation and donor-acceptor molecular orbital compatibility. In this study, we have chosen to treat only the outer-sphere mechanism for Eqn. 5, including both the rates of outer-sphere encounter complex formation and electron transfer within this encounter complex, for three reasons: (1) As will be presented, the observed oxidation rate of several of the metal ions and relevant molecular orbital compatibility arguments are suggestive of an outer-sphere mechanism. (2) Where the mechanism is unknown, the outer-sphere rate is a useful reference value for comparison against ligand exchange rates for the purpose of deducing an inner- vs. outer-sphere mechanism. (3)

Theoretical treatment of the outer-sphere mechanism is more straightforward and reliable than for the inner-sphere pathway.

Marcus (1956) developed a highly successful quantitative theory for predicting outer-sphere homogeneous electron transfer rates in solution. The basic principle relates the activation free energy (ΔG^*) for the electron transfer step to the driving force (ΔG°) and the reorganization energy (λ). In a previous study, we successfully benchmarked and adapted key quantities calculable by density functional theory (DFT) for use in the semiclassical electron transfer rate equations laid out by Marcus (Rosso and Rustad, 2000). A detailed introduction and description of this implementation are available therein and will not be repeated here, except to provide the necessary context in which we describe the extension to the current system and the several improvements that have been made.

2. THEORETICAL METHODS

2.1. Ab Initio Calculations

Structures and energies for the series of $\text{M}(\text{OH}_2)_{6-x}(\text{OH})_x^{2-x/3-x}$ ions (where $\text{M} = \text{V}, \text{Cr}, \text{Mn}, \text{Fe}, \text{Co}$ and $x = 0 - 2$) were performed unrestricted using Becke's three-parameter hybrid DFT method (UB3LYP) (Becke, 1993) with a Pople-type 6-311+G basis set in Gaussian98 (Frisch et al., 1998). UB3LYP includes both Hartree-Fock and DFT exchange and the Lee-Yang-Parr correlation functional (Lee et al., 1988) and has been shown to perform very well for these systems (Ricca and Bauschlicher, 1994; Russo et al., 1995; Martin et al., 1998; Rustad et al., 1999; Rosso and Rustad, 2000). The 6-311+G basis set consists of a Wachters-Hay 6-311G set (Wachters, 1970; Hay, 1977) with an added diffuse function ("+") (Clark et al., 1983). Clusters were optimized both in the gas-phase and when using the polarizable continuum model (PCM) of solvation by Tomasi and coworkers (Miertus et al., 1981; Miertus and Tomasi, 1982). The PCM method defines the solute cavity as a union of interpenetrating atom-centered spheres of radii chosen, in this case, using the united atom topological model. Area outside the solute cavity is defined as solvent and is modeled as a continuum of uniform dielectric constant, which may be polarized in response to dipoles in the solute. A general strategy to minimize the number of symmetry constraints used during geometry optimization was taken, allowing the clusters to deviate from octahedral symmetry and allowing for Jahn-Teller distortions. But because of the tendency of a small fraction of the PCM solvated ions and some of the hydrolyzed ions to shed water molecules from the inner hydration shell during optimization, geometry constraints were employed in the following way. The gas-phase $\text{M}(\text{OH}_2)_6^{2+/3+}$ clusters were optimized without symmetry constraints, and their respective optimized angles were fixed for the corresponding PCM optimizations while bond lengths were allowed to vary. Likewise, the optimized gas-phase $\text{M}(\text{OH}_2)_5(\text{OH})^{2+}$ angles were used to constrain all remaining clusters. All clusters were optimized in the high spin limit in accord with the predominantly observed spin configuration for the considered ions, except for $\text{Co}(\text{OH}_2)_6^{3+}$, which is observed to be low spin (Richens, 1997). The electron transfer mechanisms involving $\text{Co}(\text{OH}_2)_6^{3+}$ are still a matter of debate and may involve a spin preequilibrium step between low and high

spin states (Sutin, 1986). Therefore, for internal consistency within our metal series, we model electron transfer reactions with Co species exclusively in high spin states.

2.2. Electron Transfer Rate

Reactions of the type shown in Eqn. 5 can be viewed as the cross-reaction (defined here as having rate k_{12}) between the self-exchange electron transfer reactions for the separate metal ion (defined here as having rate k_{11}) and oxygen (defined here as having rate k_{22}) couples. In the investigation of cross-reactions, it is often instructive to first analyze the separate self-exchange reactions to determine the intrinsic reactivity of the separate couples. The Marcus equations to treat the self-exchange reactions and the cross-reactions for the outer-sphere mechanism are the same. We use the non-adiabatic formalism (pertaining to the case of weak-electronic interaction between reactants) as summarized in Marcus and Sutin (1985). A variety of formalisms and approximations exist, however; therefore, we briefly outline here the specific equations used in this study. The rate of an outer-sphere bimolecular reaction (k) such as the one shown in Eqn. 5 is a product of the equilibrium constant for the formation of the precursor complex between the reacting pair (K^{pre}) and the rate of electron transfer (k^{et}). Thus, the rate that is observable in solution depends on both the concentration of encounter complexes in solution and the rate of electron transfer in an encounter complex. This assumes that the reactions are not diffusion-limited, which can be shown to be reasonable in our case by using the Smoluchowski equation (Gardiner, 1969):

$$k_{\text{diff}} = \frac{4\pi N(D_1 + D_2)(r_1 + r_2)}{1000} \quad (6)$$

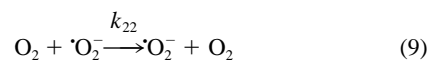
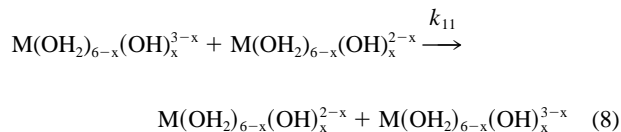
where N is Avagadro's number, D_1 and D_2 are the diffusion coefficients for the reactants in water (e.g., 7.2×10^{-6} cm²/s for Fe²⁺ (Lasaga, 1998) and 2.1×10^5 cm²/s for O₂ (Lide, 1990)) and r_1 and r_2 are their solute radii for the reactants (discussed below). Thus, for any of the reactions in this study, the slowest rates of diffusion (those not involving O₂) will be on the order of 10^{8-9} M⁻¹ s⁻¹, which is significantly faster than any of the electron transfer rates predicted here. Note that this form of the Smoluchowski equation is valid only where at least one of the reactants is uncharged (i.e., O₂).

Calculation of K^{pre} was described earlier (Rosso and Rustad, 2000) and will not be repeated here, except to mention that for the effective reaction zone thickness dR for the self-exchange reactions was taken as 0.833 Å for the metal ions (Creutz and Sutin, 1986) and 0.295 Å for oxygen (German et al., 1999). In the classical limit, k^{et} is given by (Marcus and Sutin, 1985):

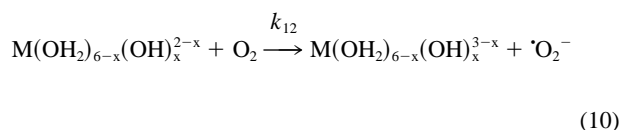
$$k^{\text{et}} = \frac{2\pi}{\hbar} H_{\text{AB}}^2 \frac{e^{-(\Delta G^\circ + \lambda)^2/4\lambda RT}}{\sqrt{4\pi\lambda RT}} \quad (7)$$

where \hbar is Planck's constant, H_{AB} is the electronic matrix element describing the coupling of the electronic state of the reactants to that of the products, ΔG° is the free energy of reaction corrected for the work to bring the reactants together and the products together in the encounter complex (see below), λ is the energy to reorganize the nuclear coordinates of the reactants and surrounding solvent molecules into the con-

figuration of the products, R is the gas constant, and T is the temperature (taken as 298.15 K throughout this study). We use this equation to calculate the rates of self-exchange for each of the $\text{M}(\text{OH}_2)_{6-x}(\text{OH})_x^{2-x/3-x}$ couples and for the O₂^{0/1-} couple, as well as for the oxidation cross-reaction between the two couples. The self-exchange rate of the former $k_{11} = K_{11}^{\text{pre}} k_{11}^{\text{et}}$ and the self-exchange rate of the latter $k_{22} = K_{22}^{\text{pre}} k_{22}^{\text{et}}$ are calculated for the reactions:



The cross-reaction rates $k_{12} = K_{12}^{\text{pre}} k_{12}^{\text{et}}$ are calculated for the reactions:



H_{AB}^{11} has been calculated for $\text{M}(\text{OH}_2)_6^{2+/3+}$ couples by fitting relevant experimental thermodynamic data with analytic functions to generate accurate potential energy surfaces (Bu et al., 1998). We calculate H_{AB}^{11} values for all $\text{M}(\text{OH}_2)_{6-x}(\text{OH})_x^{2-x/3-x}$ couples using (Newton and Sutin, 1984):

$$H_{\text{AB}}^{11} = H_{\text{AB}}^0 \exp[-\beta(r - r_0)/2] \quad (11)$$

where H_{AB}^0 and r_0 were taken as (Bu et al., 1998) 30.9 cm⁻¹ and 6.2 Å for all V ions, 96.5 cm⁻¹ and 5.3 Å for all Cr ions, 76.9 cm⁻¹ and 6.85 Å for all Mn ions, 64.0 cm⁻¹ and 6.2 Å for all Fe ions, and 54.9 cm⁻¹ and 5.8 Å for all Co ions, respectively, and $\beta = 1.2$ Å⁻¹ (Newton and Sutin, 1984; Marcus and Sutin, 1985). For the O₂^{0/1-} couple, H_{AB}^{22} has been evaluated explicitly from semiempirical calculations, including solvation for three different encounter configurations (German et al., 1999). We take the mean of the three values at their respective optimal interreactant distances. For the cross-reactions, we estimate H_{AB}^{12} from the self-exchange values described above using (Sutin, 1986):

$$H_{\text{AB}}^{12} = (H_{\text{AB}}^{11} H_{\text{AB}}^{22})^{1/2} \quad (12)$$

Likewise, dR for the cross-reaction is taken as the geometric mean of dR s for the separate self-exchange reactions.

The energy ΔG° is the free energy change for electron transfer in the encounter complex at the optimal separation distance r and therefore is not the same as the overall free energy change of reaction ΔG° . The former is related to the latter by (Marcus and Sutin, 1985):

$$\Delta G^{\circ'} = \Delta G^\circ - w_R + w_P \quad (13)$$

where w_R and w_P are the work necessary to bring the reactants and products together, respectively. Because the electrostatic interactions between the ions can be large for the reactions in this study, we use an approximate equation to calculate the

electrostatic work terms, which depends on the formal charges on the interacting species with corrections for the solution ionic strength, as described in Weaver and Lee (1980) and used successfully elsewhere (Rosso and Rustad, 2000). For the self-exchange reactions $\Delta G^\circ = 0$ and, because the reactant charges are always the same as the product charges, the work terms cancel and therefore $\Delta G^\circ = 0$ also (but w_R is still used in the calculation of K^{pre}). For the cross-reactions where data are already available, we use experimental estimates for ΔG° . For the hexaquo metal ions, we used reduction potentials listed in Lide (1990). For their hydrolysis counterparts, we used stability constants found in Smith and Martell (1979) with the reduction potentials of the hexaquo ions to compute the reduction potentials of the hydrolysis species. For hydrolysis species, where no experimental thermodynamic data could be found (dihydroxo V, Cr, and Co), we calculated ΔG° from the ab initio total energies for the optimized structures, including solvation free energy terms from the PCM model, and modified them using a TΔS entropy correction estimated from experimental S° data for $\text{Fe}(\text{OH}_2)_6^{2+/3+}$ (298.15 K, 1 bar standard state) (Wagman et al., 1968) and a relativistic correction (~ 0.1 eV) estimated in Li et al. (1996). The equilibrium constant for the overall reaction (K_{12}) was estimated from ΔG° using $\ln K_{12} = -\Delta G^\circ/RT$.

The reorganization energy λ can be taken as the sum of an inner-sphere term (λ_{is}) and an outer-sphere term (λ_{os}) (Marcus and Sutin, 1985). For the self-exchange reactions, we calculate λ_{is} using a four-point energy scheme (Klimkans and Larsson, 1994), using the ab initio total energies of the ground and excited state partner molecules as was done in Rosso and Rustad (2000), except in this case we improve the estimate by including solvation free energy corrections from the PCM model. We calculate λ_{os} using the continuum expression by Marcus (1956). For cross-reactions, Marcus also showed that without a significant loss of accuracy (Marcus and Sutin, 1985)

$$\lambda_{12} = \frac{\lambda_{11} + \lambda_{22}}{2} \quad (14)$$

We use this equation to calculate λ_{12} for the cross-reactions using the reorganization energies calculated for the self-exchange reactions.

Radii for the metal ions were taken as the sum of the average optimized M–O bond lengths and an adjustment parameter (Rosso and Rustad, 2000). In Rosso and Rustad (2000), the adjustment parameter was determined by calibrating theoretical k_{11} 's against experiment for $\text{M}(\text{OH}_2)_6^{2+/3+}$ complexes. It is meant to account for the “actual” size of the solute cavity beyond the average M–O bond lengths. The 0.56 Å value determined therein was based on gas-phase calculations. It was re-evaluated in the current study using the PCM DFT calculations and determined to be 0.90 Å, which is used here throughout for all metal ions. Radii for the O_2 and O_2^- species were taken as the spherical radii corresponding to the volume of the solute cavities estimated by the PCM model (2.12 and 2.01 Å, respectively). The separation distances r for the metal ions were taken as the sum of the average M–O bond lengths and twice the adjustment parameter 0.90 Å, whereas 2.8 Å was used for the $\text{O}_2^{0/1-}$ couple based on the work of German et al. (1999). For the cross-reactions, r was taken as the sum of the relevant

Table 1. Calculated electron transfer rate parameters for self-exchange reactions of the $\text{M}(\text{OH}_2)_{6-x}(\text{OH})_x^{2-x/3-x}$ couples, based on density functional calculations using the PCM solvation model. The work term w_R is calculated for $\mu = 0.0$ M. Effective electron transfer distances r are ~ 6.0 Å. Values of H_{AB}^1 for the hexaquo ions were derived from Bu et al. (1998) and applied respectively to each species of a particular metal ion. For the dihydroxo species, the calculated lowest energy isomer (*cis*- vs. *trans*-) for each metal is given in the text.

	V	Cr	Mn	Fe	Co
$\text{M}(\text{OH}_2)_6^{2+/3+}$					
λ_{is} (eV)	1.23	2.58	2.40	0.82	0.93
λ_{os} (eV)	1.34	1.35	1.34	1.34	1.36
λ (eV)	2.57	3.92	3.74	2.16	2.29
$\log k_{11}^{\text{et}}$ (s^{-1})	0.45	-4.82	-3.45	2.86	1.99
w_R (kJ/mol)	17.9	18.0	17.8	17.9	18.1
$\log K_{11}^{\text{pre}}$ (M^{-1})	-3.79	-3.80	-3.77	-3.79	-3.84
$\log k_{11}$ ($\text{M}^{-1} \text{s}^{-1}$)	-3.34	-8.62	-7.23	-0.93	-1.85
$\text{M}(\text{OH}_2)_5(\text{OH})^{1+/2+}$					
λ_{is} (eV)	0.94	2.27	1.88	0.94	1.02
λ_{os} (eV)	1.33	1.34	1.33	1.33	1.35
λ (eV)	2.28	3.60	3.21	2.28	2.38
$\log k_{11}^{\text{et}}$ (s^{-1})	1.71	-3.47	-1.19	2.33	1.61
w_R (kJ/mol)	5.9	6.0	5.9	5.9	6.0
$\log K_{11}^{\text{pre}}$ (M^{-1})	-1.69	-1.69	-1.68	-1.69	-1.71
$\log k_{11}$ ($\text{M}^{-1} \text{s}^{-1}$)	0.02	-5.17	-2.87	0.64	-0.11
<i>trans</i> - $\text{M}(\text{OH}_2)_4(\text{OH})_2^{0/1+}$					
λ_{is} (eV)	1.51	1.93	1.70	0.91	0.77
λ_{os} (eV)	1.33	1.34	1.32	1.33	1.34
λ (eV)	2.84	3.27	3.02	2.24	2.11
$\log k_{11}^{\text{et}}$ (s^{-1})	-0.71	-2.03	-0.41	2.50	2.75
w_R (kJ/mol)	0.0	0.0	0.0	0.0	0.0
$\log K_{11}^{\text{pre}}$ (M^{-1})	-0.65	-0.65	-0.64	-0.64	-0.65
$\log k_{11}$ ($\text{M}^{-1} \text{s}^{-1}$)	-1.35	-2.67	-1.05	1.86	2.10
<i>cis</i> - $\text{M}(\text{OH}_2)_4(\text{OH})_2^{0/1+}$					
λ_{is} (eV)	1.24	2.30	2.21	1.19	1.03
λ_{os} (eV)	1.36	1.37	1.38	1.36	1.35
λ (eV)	2.60	3.67	3.59	2.55	2.38
$\log k_{11}^{\text{et}}$ (s^{-1})	0.45	-3.61	-2.60	1.27	1.60
w_R (kJ/mol)	0.0	0.0	0.0	0.0	0.0
$\log K_{11}^{\text{pre}}$ (M^{-1})	-0.65	-0.64	-0.64	-0.65	-0.65
$\log k_{11}$ ($\text{M}^{-1} \text{s}^{-1}$)	-0.20	-4.25	-3.24	0.63	0.94

M–O bond length and 0.56 Å and the spherical radius for relevant oxygen species.

3. RESULTS AND DISCUSSION

3.1. Metal Ion Self-Exchange

It is valuable to first discuss the self-exchange reactions for the separate couples, because the molecular properties controlling these reactions also influence the rate of the cross-reactions between the metal ions and oxygen. Calculated electron transfer parameters for the outer-sphere metal ion self-exchange reactions are given in Table 1. Within an isostructural series, the single most important parameter controlling k_{11} is λ_{is} . The wide variation in this term reflects the large differences in the bond length changes required for the reactants to distort into the structural conformation of the products. The energy required to accomplish this distortion is strongly affected by the type of electron accepting d-orbital on the metal atom. The reduction of both Cr and Mn involves the transfer of an electron into the e_g^* orbitals, which point towards the ligands (i.e., σ^* -character). This causes substantial M–O bond weakening in the reduced complex. Therefore, the bond lengths in the reduced complex

are significantly longer than in the oxidized counterpart, leading to large values of λ_{is} and thus slower k_{11} 's. In contrast, Fe, V, and Co accept the electron into non-bonding t_{2g} orbitals pointing into the voids between the ligands (i.e., π -character), equating to smaller required changes in M–O bond lengths, lower λ_{is} energies, and therefore faster k_{11} 's.

These electron transfer reactions are typified by weak electronic coupling (non-adiabatic), and the variability of H_{AB}^{11} is in the range 30 to 100 cm^{-1} (Creutz and Sutin, 1986). Because k_{et} depends on the square of H_{AB} (see "Theoretical Methods" section), differences in the electronic coupling within this series of metals can adjust the rate by 2 orders of magnitude. Therefore, H_{AB} is also clearly an important factor affecting the rates within an isostructural series.

We note here that Table 1 reports parameters for both the *trans*- and *cis*- isomers of the dihydroxo species. The computed total energies suggest that the *trans*- isomers of V and Fe are energetically favored over their *cis*- counterparts, and vice versa for Cr, Mn, and Co. This was found to be true for both the oxidized and reduced forms. To our knowledge, there are no experimental data with which to compare the relative stabilities of the isomers for these metals. This is possibly due to the difficulties in isolating their monomers in solution, especially the oxidized forms that quickly drop out of solution as precipitates (Richens, 1997). The calculations provide some basis for assuming which isomer will dominate the speciation of the dihydroxo forms. Therefore, all ensuing results and discussions regarding the dihydroxo species are with respect to the *cis*- isomers of V and Fe and the *trans*- isomers of Cr, Mn, and Co.

Comparing now k_{11} 's for any particular metal as it goes through hydrolysis steps, the variability of λ_{is} also strongly affects the rates. But in contrast to the trends within isostructural series, the work required to bring the reactant species together varies substantially, with w_R decreasing as the reactants are incrementally hydrolyzed, thereby lowering the net positive charge on the metal ions and decreasing the Coulombic repulsion that must be overcome to form an encounter complex (Table 1). This has a large stabilizing effect on encounter complex formation, reflected in significant increases in K_{11}^{pre} and therefore k_{11} . Figure 1 graphically shows the increase in k_{11} with hydrolysis observed in a regular step-wise fashion for all but two of the steps (monohydroxo- to dihydroxo-V and monohydroxo- to dihydroxo-Mn). The work term is therefore predicted to be a primary factor in the rate increase observed for these metals as they are hydrolyzed in solution. In general, this is likely to hold true regardless of whether the electron transfer mechanism is inner- or outer-sphere, because encounter complex formation is a prerequisite in both mechanistic pathways.

The most studied of the metal ions have been the hexaquo complexes, and experimental data are available for these species to compare with the calculations. In Table 2, typical observed rates are compared with calculated rates, which have been adjusted for the specific ionic strength conditions reported in the experiments. It should be noted that observed rates can vary widely in the literature, depending on how the rate was determined. Self-exchange rates for transition metal ions can sometimes be measured directly using isotopic labeling, nuclear magnetic resonance, or electron paramagnetic resonance methods (Lappin, 1994). More often, the self-exchange rates

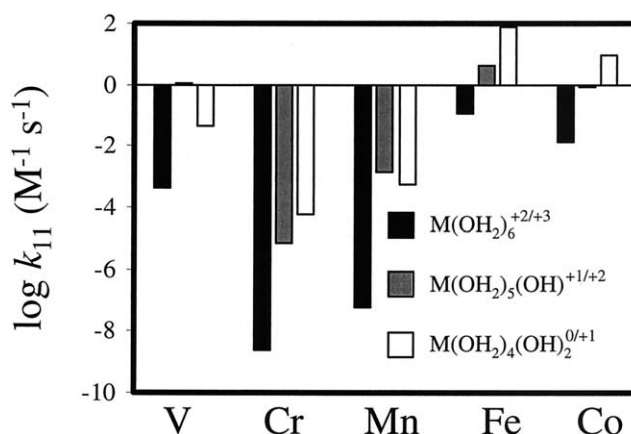


Fig. 1. Calculated self-exchange rates (k_{11}) for the 15 metal ion species treated in this study. In general, Mn and Cr self-exchange reactions are slower, and V, Fe, and Co are faster. Hydrolysis increases the rate.

are determined indirectly by application of the Marcus cross-relation to a cross-reaction involving the self-exchange couple of interest and another couple having an independently determined self-exchange rate. The latter approach is susceptible to failure if either the chosen cross-reaction itself or either of the corresponding self-exchange reactions follows an inner-sphere pathway, or if the degree of non-adiabaticity is different between the self-exchange and cross-reactions. To avoid these uncertainties, we have chosen directly measured observed values for comparison with our calculated rates in Table 2. The agreement is satisfactory for V and excellent for Fe, and Co, whereas the calculated rates for Cr and Mn are 1.5–2.0 orders of magnitude slower than the observed rates. The agreement found for V, Fe, and Co can be taken as evidence for an outer-sphere mechanism. Molecular orbital arguments pertaining to V, Fe, and Co self-exchange reactions support this view. These electron transfers occur between donor and acceptor orbitals of π symmetry. Not only do the π - to π - orbital electron transfers require smaller bond length changes, but π -orbitals are also more diffuse and therefore have a higher propensity for good overlap at the longer metal-metal separations often required in outer-sphere encounter complexes (Luther, 1990). The assignment of an outer-sphere mechanism for the well-studied hexaquo $\text{Fe}^{2+/3+}$ self-exchange reaction is consistent with several previous investigations (Brunschwig et al., 1980, 1982; Tembe et al., 1982; Logan and Newton, 1983; Jolley et al., 1990). However, for self-exchange reactions involving hydroxo-hexaquo species of Fe, significantly less is known from experiment, but evidence does exist for an inner-sphere pathway via an OH^- ligand bridge (Jolley et al., 1990). In general, the predisposition of hydrolysis species towards an inner-sphere mechanism derives from the conjugate-base mechanism of ligand substitution, whereby hydrolyzed metal species are labilized towards ligand exchange and hence towards the inner-sphere mechanism.

The disagreement found for hexaquo Cr and Mn, where the observed rate is faster than predicted for an outer-sphere pathway (Table 2), is indirect evidence for an inner-sphere pathway operating in the self-exchange reactions of Cr and Mn. The inner-sphere tendencies of $\text{Cr}(\text{OH}_2)_6^{2+}$ have been observed in a

Table 2. Calculated vs. observed $\log k_{11}$ ($M^{-1} s^{-1}$) for self-exchange electron transfer reactions of the hexaquo ions corrected for the ionic strengths used in the experiments. All observed values are derived from direct measurement of the self-exchange rate, unless otherwise noted.

$M(OH_2)_6^{2+/3+}$	V $\mu = 2.0^a$	Cr $\mu = 1.0^b$	Mn $\mu = 3.0^c$	Fe $\mu = 0.6^d$	Co $\mu = 3.0^e$
Calculated (this study)	-1.04	-6.55	-4.81	0.95	0.60
Observed	-2.00	-4.70	-3.52	0.62	0.52

^a Krishnamurty and Wahl (1958).

^b Anderson and Bonner (1954).

^c Diebler and Sutin (1964) determined this rate from application of Marcus theory to the cross-reaction between Mn^{3+} and Fe^{2+} . Note, subsequent studies have shown that $\log k_{11}$ for $Mn(OH_2)_6^{2+/3+}$ varies widely between -2.4 to -9 , depending on the cross-reaction studied (Macartney and Sutin, 1985) (see text for more detailed discussion).

^d Silverman and Dodson (1952).

^e Habib and Hunt (1966).

variety of redox reactions and are attributed to the σ^* character of its donor d-orbital, a fast water exchange rate that increases the chance of forming bridged encounter complexes ($k_{ex} \sim 10^9 s^{-1}$) and the electronic stability of the symmetric occupation of the t_{2g} orbitals in the $Cr(OH_2)_6^{3+}$ product (Richens, 1997). Using isotopic labeling methods, measurements of the $Cr(OH_2)_6^{2+/3+}$ self-exchange rate as a function of solution pH led Anderson and Bonner (1954) to conclude that the reaction proceeds predominantly by a hydroxo-bridged inner-sphere path. $Mn(OH_2)_6^{2+}$ is also a σ^* donor and is labile ($k_{ex} \sim 10^7 s^{-1}$) but is stabilized towards oxidation by its symmetric d^5 configuration and large reorganization energy (Rosso and Rustad, 2000). But we note that there is very little agreement in the literature regarding the self-exchange rate of $Mn(OH_2)_6^{2+/3+}$. Early attempts at direct measurement of k_{11} for this species using isotopic labeling by Diebler and Sutin (1964) were unsuccessful, and therefore all available estimates are based on the application of Marcus relations to cross-reactions involving $Mn(OH_2)_6^{2+/3+}$. For reasons cited above, this strategy has met with varying degrees of success as was highlighted in a more recent study by Macartney and Sutin (1985) where it was shown that k_{11} can vary from $10^{-2.4}$ to $10^{-9} M^{-1} s^{-1}$, depending on the nature of the reactant couple used in the cross-reaction. In that study, a best estimate of $k_{11} = 10^{-3} - 10^{-5} M^{-1} s^{-1}$ for $Mn(OH_2)_6^{2+/3+}$ was presented based on an improved Marcus model. This estimate is in line with our prediction for the outer-sphere pathway, but because of the lack of overall consistency in the observed rates, the evidence is not compelling enough for us to conclude that $Mn(OH_2)_6^{2+/3+}$ self-exchange follows an outer-sphere pathway. Rather, based on the results for Cr and the molecular orbital arguments presented above, we single out the σ^* donors Cr and Mn as likely inner-sphere reactants during self-exchange.

3.2. Oxygen Self-Exchange

Calculated Marcus parameters for the oxygen self-exchange reaction in water are given in Table 3. Bond length differences between O_2 and O_2^- , as determined by the DFT calculations, are predicted to be relatively large (1.254 and 1.402 Å, respectively), leading to a large λ_{is} , given the simplicity of the structure. The acceptor orbital in O_2 is one of the degenerate half-filled π^* orbitals leading to weakening of the O-O double bond upon reduction and instability in the superoxide radical product. The π^* to π^* match between donor/acceptor orbital

symmetries makes this reaction a relatively fast outer-sphere exchange. This is, in large part, the justification for attributing an outer-sphere mechanism for the self-exchange electron transfer reactions for the $O_2^{0/1-}$ couple (Ohta and Morokuma, 1987; Bu and Liu, 1999; Bu et al., 1999; German et al., 1999). Estimates of k_{22} based on the application of Marcus cross-relation equations to experimental cross-reaction rates have varied 16 orders of magnitude (Lind et al., 1989). Likely explanations include the failure to identify the operation of inner-sphere pathways or to account for variability in the non-adiabatic behavior in the cross-reactions, equivalent to problems cited above for estimating metal ion self-exchange rates from the Marcus cross-relation. Of the reported k_{22} 's generated in this way, estimates in the range 1 to $1000 M^{-1} s^{-1}$ have been the most accepted based on the results of Espenson and coworkers (Zahir et al., 1988) and Stanbury et al. (1980). Nevertheless, it is clear that direct measurement of k_{22} is preferable, rather than deducing k_{22} using the Marcus cross-relation. The only direct measurement available to our knowledge is by Lind et al. (1989), where use of isotopic labeling indicated that $k_{22} = 450 \pm 160 M^{-1} s^{-1}$. Our calculations based on DFT clusters and PCM solvation, and r , H_{AB}^{22} , and dR , calculated explicitly using semiempirical methods (German et al., 1999), arrive at $k_{22} = 360 M^{-1} s^{-1}$. The German et al. (1999) study predicts the range 28 to $296 M^{-1} s^{-1}$, depending on the orientation of the reactants in the encounter complex, and other recent MP2 estimates are one order of magnitude less (Bu and Liu, 1999; Bu et al., 1999). The good agreement between our prediction, the German et al. (1999) study, and the

Table 3. Calculated electron transfer rate parameters for the $O_2^{0/1-}$ self-exchange reaction in solution based on density functional calculations using the PCM solvation model. The effective electron transfer distance r is 2.8 Å and $H_{AB}^{22} = 120.5 cm^{-1}$, and $dR = 0.295 Å$ (German et al., 1999) (see "Methods" section). The only available directly observed experimental rate is given for comparison (Lind et al., 1989).

	$O_2^{0/1}$
λ_{is} (eV)	0.98
λ_{os} (eV)	1.02
λ (eV)	2.00
$\log k_{22}^{et}$ (s^{-1})	3.98
w_R (kJ/mol)	0.0
$\log K_{22}^{pre}$ (M^{-1})	-1.75
$\log k_{22}$ ($M^{-1} s^{-1}$)	2.22
Exp. $\log k_{22}$ ($M^{-1} s^{-1}$)	2.65

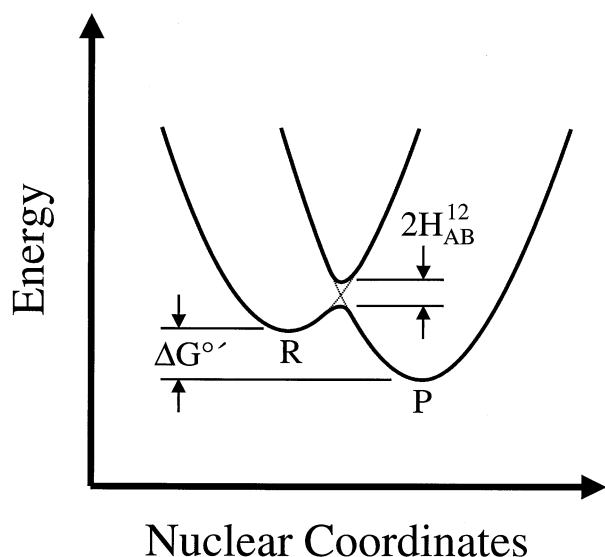


Fig. 2. Depiction of the potential energy surface for the reactants (parabola marked “R”) and products (parabola marked “P”) as a function of the nuclear configuration for an exothermic (ΔG°) oxidation cross-reaction. Weak mixing between the reactant orbitals is represented by the splitting in the intersection region and quantified by H_{AB}^{12} .

direct measurement (Lind et al., 1989) lead us to conclude that our k_{22} is satisfactory.

3.3. Metal Ion Oxidation Rates

The parameters controlling k_{12}^{et} for the bimolecular oxidation cross-reaction as shown in Eqn. 5 derive directly from the

parameters for the separate self-exchange reactions, except for what is now a non-zero ΔG° (Fig. 2). One of the triumphs of Marcus theory is its ability to accurately predict outer-sphere cross-reaction rates using only a knowledge of the quantities controlling the self-exchange rates of the separate redox couples. This normally pertains to the condition where $|\Delta G^\circ| < \lambda$, as is the case for all cross-reactions considered in this study. Having calculated λ for the cross-reaction from the mean of those for the self-exchange reactions, and similarly estimating H_{AB}^{12} , an estimate of the overall free energy change on going from products to reactants is required (ΔG°). When corrected for work terms, ΔG° is used in the equation to predict k_{12}^{et} (see “Theoretical Methods” section). Because of the difficulties in calculating quantities such as solution phase reduction potentials using ab initio calculations (e.g., Li et al., 1996), it is generally desirable to rely on experimental estimates, where available, for this quantity. We have done so for all but the dihydroxo species of V, Cr, and Co. The others are not stable species (Richens, 1997), and, to our knowledge, experimental data do not exist. Therefore, we used the density functional total energies to estimate ΔG° for these species (see “Theoretical Methods” section). The ability to do so accurately is crucial for electron transfer reactions where experimental estimates of ΔG° are unknown.

Calculated rate parameters for the cross-reactions are given in Table 4. In contrast to the metal self-exchange reactions, because the reactant O_2 is uncharged and therefore w_R is zero, K_{12}^{psc} becomes approximately the same for any of the cross-reactions. Also, w_P becomes an important term, because it is used to correct ΔG° to ΔG° . The work term w_P varies little within an isostructural series, but, as for the metal self-exchange

Table 4. Calculated electron transfer rate parameters for the bimolecular oxidation cross-reactions (see Eqn. 5) based on DFT calculations using the PCM solvation model. Experimental data were used to estimate ΔG° for all but the dihydroxo V, Cr, and Co species, where data are not available so DFT total energies were used. The work term w_P is calculated for $\mu = 0.0$ M. Because $w_R = 0$, K_{12}^{psc} is approximately the same for all of the reactions ($\log K_{12}^{\text{psc}} \sim -0.94$). The effective electron transfer distance r is ~ 4.9 Å. For the dihydroxo metal species, the parameters given are for the oxidation of the lowest energy isomer (see text).

	V	Cr	Mn	Fe	Co
$M(OH_2)_6^{2+/3+}$					
λ (eV)	2.29	2.96	2.87	2.08	2.14
H_{AB}^{12} (cm^{-1})	65.9	89.5	125.6	95.2	79.8
w_P (kJ/mol)	-10.8	-10.9	-10.8	-10.8	-10.9
ΔG° (kJ/mol)	-20.5	-35.0	153.2	78.9	181.2
$\log K_{12}$	1.69	4.23	-28.74	-15.72	-33.64
$\log k_{12}^{\text{et}}$ (s^{-1})	3.92	2.45	-16.88	-4.86	-19.83
$\log k_{12}$ ($\text{M}^{-1} \text{s}^{-1}$)	2.97	1.50	-17.82	-5.80	-20.78
$M(OH_2)_5(OH)^{1+/2+}$					
λ (eV)	2.14	2.80	2.60	2.14	2.19
H_{AB}^{12} (cm^{-1})	65.4	88.6	124.2	94.2	78.9
w_P (kJ/mol)	-7.2	-7.2	-7.2	-7.2	-7.2
ΔG° (kJ/mol)	-36.8	-39.9	93.0	40.8	132.5
$\log K_{12}$	5.19	5.73	-17.55	-8.41	-24.47
$\log k_{12}^{\text{et}}$ (s^{-1})	5.78	3.48	-8.26	-0.78	-12.45
$\log k_{12}$ ($\text{M}^{-1} \text{s}^{-1}$)	4.83	2.54	-9.20	-1.72	-13.41
$M(OH_2)_4(OH)_2^{0/1+}$					
λ (eV)	2.42	2.81	2.77	2.12	2.19
H_{AB}^{12} (cm^{-1})	65.1	87.4	122.9	93.0	78.2
w_P (kJ/mol)	-3.6	-3.6	-3.6	-3.6	-3.6
ΔG° (kJ/mol)	-159.4	-161.3	30.9	0.9	19.9
$\log K_{12}$	27.30	27.62	-6.04	-0.79	-4.12
$\log k_{12}^{\text{et}}$ (s^{-1})	10.82	10.11	-2.18	3.16	0.96
$\log k_{12}$ ($\text{M}^{-1} \text{s}^{-1}$)	9.88	9.17	-3.12	2.22	0.01

reactions, it varies significantly with the hydrolyzed state of the metal ions. The quantities λ , H_{AB}^{12} , and ΔG° are the principal parameters causing the variability of k_{12}^{et} within an isostructural series. The trend of large relative λ 's for Cr and Mn is preserved in the cross-reactions, because they are simply being modified by a constant value. But λ can no longer be correlated one-to-one with the resulting rate, as it can be seen that ΔG° significantly modifies the outcome. For example, the slowness predicted for $Mn(OH_2)_6^{2+}$ oxidation by O_2 is due to both a large λ and large positive ΔG° , whereas for $M(OH_2)_4(OH)_2^0$ where λ is nearly identical, the rate is predicted to be 15 orders of magnitude faster because in this case ΔG° is substantially shifted towards exothermicity.

In this regard, the accuracy of the estimates for ΔG° based on the DFT total energies is satisfactory overall. For the oxidation of the hexaquo ions, for which experimental reduction potentials are well known, the standard deviation of ΔG° from experimental estimates is 25 kJ/mol, including all ions except Cr, where the performance was less than satisfactory. The best agreement is obtained for Mn (-22%), Fe (-2%), and Co (+8%). This means that reliance on the DFT total energies, as has been done for three of the 15 considered metal ions, introduces an uncertainty of up to ~ 0.2 eV into the $\Delta G^\circ + \lambda$ part of the k^{et} equation, where λ varies on the order of 2 to 3 eV. Although for Cr the ΔG° agreement is anomalously poor, it is unlikely that better performance can be expected from the UB3LYP/6-311+G/PCM method for V, Mn, Fe, and Co, given that the second hydration shell has not been treated explicitly (Li et al., 1996) and thermochemical parameters such as zero-point and vibrational energies have been ignored for the inner-sphere of the complex. But for the majority of the metal ions, because we have used experimental ΔG° 's, the accuracy is assumed to be much better.

Building on the molecular orbital arguments pertaining to the self-exchange reactions noted earlier, the comparison must now be made between the metal donor orbital symmetries and the π^* acceptor orbital of O_2 . The σ^* donor orbitals for both Cr and Mn are a poor symmetry match with the π^* acceptor orbital of O_2 , specifically for outer-sphere electron transfers (Luther, 1990). But this combination is amicable to the formation of an inner-sphere adduct such as $[M(OH_2)_5(O_2)]^{2+}$. In this case, the O_2 molecule is exchanged into the one of the sixfold coordinate sites with one of its oxygen atoms binding directly to the metal center (Bakac et al., 1995). The oxidation of $Cr(OH_2)_6^{2+}$ has been observed to occur through via the adduct $[Cr(OH_2)_5(O_2)]^{2+}$ with $k_{12} = 1.6 \times 10^8 \text{ M}^{-1} \text{ s}^{-1}$, the K_{12}^{pre} of which has been estimated to be $6 \times 10^{11} \text{ M}^{-1}$ (Sellers and Simic, 1976). These rates are significantly faster than the predicted outer-sphere oxidation rates (Table 4). Thus, an inner-sphere pathway has been both experimentally established and supported by our assessment of the outer-sphere rate for Cr oxidation by O_2 .

The dominant pathway for Mn oxidation is less well documented. To the best of our knowledge, Mn- O_2 inner-sphere adducts have not been directly observed during homogeneous oxidation of Mn aquo or hydroxo ions by O_2 . However, their formation has been viewed as necessary based on the form of the rate law, and isotopic labeling studies showing that a large fraction of oxygen in resulting solid phase oxidation products is derived from O_2 (Luther, 1990). But such a pathway is also

somewhat counterintuitive given the tremendously sluggish oxidation rate known for $Mn(OH_2)_6^{2+}$, while at the same time, the extreme lability of water molecules in the inner coordination shell equates to very high probabilities of forming inner-sphere encounter complexes with O_2 . Close-range electron transfers through bonds such as Mn^{2+} -O-O should be much faster than the proximal "through-space" electron transfers as entailed by the outer-sphere treatment. Luther (1990) has argued that the reducing power of the Mn center is not sufficient unless either water ligands are replaced by hydroxyls which donate electron density to the Mn or the octahedral ligand field around the Mn is decomposed. Indeed, the very unfavorable ΔG° for the Mn hexaquo ion oxidation reaction (152.4 kJ/mol) is reduced significantly by hydrolysis (Table 4). Thus, although direct evidence of an inner-sphere Mn^{2+} oxidation reaction does not seem to exist, molecular orbital theory supports an inner-sphere pathway.

On the other hand, molecular orbital arguments pertaining to the oxidation reactions for Fe, V, and Co suggest that these metals are intrinsically better equipped to follow an outer-sphere pathway. The π symmetry of the donor orbitals is a better match with the π^* acceptor orbital on O_2 . However, inner-sphere exceptions to this molecular orbital argument are implied to exist from experiments of the oxidation of V^{2+} by O_2 because of the vanadium-oxygen bonding found in the oxidation products such as the vanadyl ion (Swinehart, 1965; Rush and Bielski, 1985). The oxidation mechanism of aqueous Fe^{2+} by O_2 was diagnosed as outer-sphere previously (Wehrli, 1990). A comparison of our predicted species-specific rate constants for the outer-sphere pathway against a sampling of recent rate constants derived from rate law fits to experimental data is given in (Table 5) For $Fe(OH_2)_6^{2+}$, the agreement is remarkably good considering that the scatter in the experimental data is on the order of magnitude scale. It is also remarkable considering that the Marcus theory predictions are specifically for a single elementary reaction step, usually not easily accessible by experiment, and require only a handful of molecular scale parameters for each of the separated component reaction couples. The good agreement for this species is evidence in support of an outer-sphere mechanism for the oxidation of $Fe(OH_2)_6^{2+}$ by O_2 . However, the predicted rates of oxidation of the hydrolysis species of Fe clearly are significantly slower than observed (Table 5). The predicted outer-sphere oxidation rate for $Fe(OH_2)_5(OH)^{1+}$ is ~ 2 to 3 orders of magnitude slower than observed, and for $Fe(OH_2)_4(OH)_2^0$ the difference becomes ~ 4 orders of magnitude. This is indirect evidence that the hydrolysis species of Fe^{2+} are oxidized by an inner sphere pathway, as postulated by Luther (1990). Although to the best of our knowledge, no direct evidence of inner-sphere complexation exists for the oxidation step in this system, Fe^{2+} -O-O bonding is found, for example, at the active site in oxyhemoglobin (Goddard and Olafson, 1975; Olafson and Goddard, 1977; Scherlis and Estrin, 2002), lending credence to the inner-sphere oxidation mechanism for the hydrolysis species of Fe^{2+} by O_2 .

Collectively for the oxidation cross-reactions for the 15 metal ions considered, the rate behavior derives primarily from the interplay between the quantities λ and ΔG° . On the condition that $|\Delta G^\circ| \ll \lambda$, the Marcus formalism predicts a linear relationship between $\log k_{12}$ and $\log K_{12}$. More generally, over

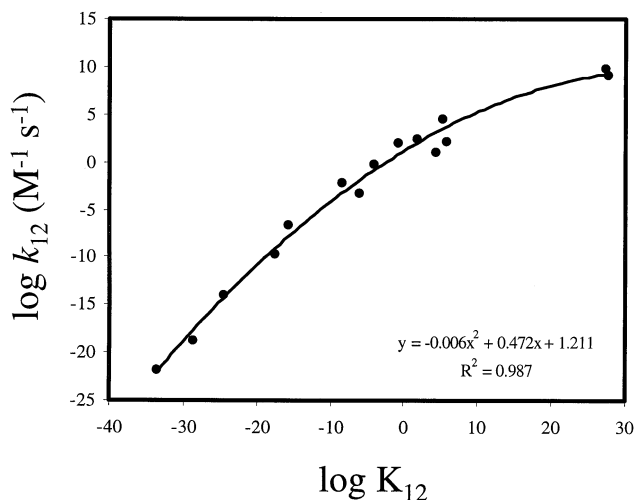


Fig. 3. Free energy relationship plot from calculated values of $\log k_{12}$ and $\log K_{12}$. The trend is substantially curved over the wide $\log K_{12}$ range considered, consistent with the Marcus formalism.

a wide range of ΔG° , plots of the same are curved with a local slope (α) defined by (Marcus and Sutin, 1985):

$$\alpha = 0.5(1 + \Delta G^\circ/\lambda) \quad (15)$$

A plot of $\log k_{12}$ vs. $\log K_{12}$ showing that the behavior is substantially curved is shown in Figure 3. In the linear approximation, the slope is close to 0.5, as is commonly observed (Marcus and Sutin, 1985). This may be compared with another estimate of a slope of 1, which is based on a Marcus analysis of experimental rates and $\log K$'s for the oxidation of iron, copper, and vanadium ions (Wehrli, 1990). The $\log K$ range considered was narrower than in this study and located in the negative $\log K$ region of our free-energy relationship plot. In that region, our predicted slope approaches 0.8 and is therefore not that different from the Wehrli estimate. In our assessment, the agreement is satisfactory, given the significantly different approaches employed in the two studies. But because we have shown that the relationship is substantially curved, it may be more appropriate to characterize the free energy relationship in terms of α . When α is plotted for each metal ion, one can easily

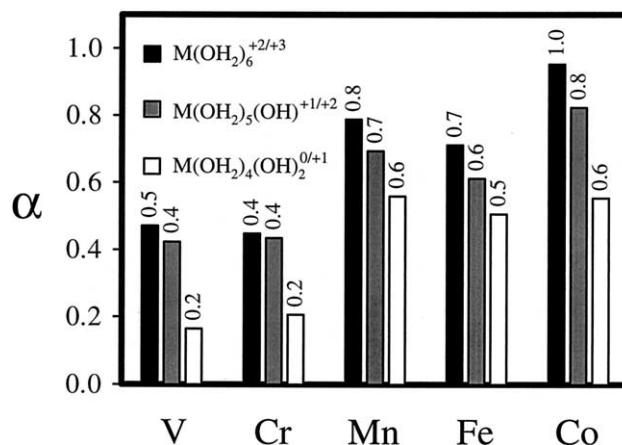


Fig. 4. Calculated values for the local slope α for the metal oxidation reactions.

see that subtrends exist in the oxidation rates (Fig. 4). For any particular metal, the hexaquo ions exhibit the largest slopes, and the dihydroxo ions exhibit the smallest slopes. This reflects the large effect of modifying ΔG° due to hydrolysis while λ is less affected.

4. CONCLUSIONS

Theoretical treatment of the oxidation of geochemically important metal aquo and hydroxo ions by oxygen has uncovered the principal physicochemical quantities that control the oxidation rate for the outer-sphere pathway. Within an isostructural ion series, one key parameter controlling the oxidation rate is the inner-sphere component of the reorganization energy λ_{is} . This term varies widely among the five different metal atoms because of the large differences in bond length changes required in the metal complex for the reduced form to distort into the conformation of the oxidized form. This in turn derives primarily from the nature of the electron accepting d-orbital on the metal atom. In contrast, the outer-sphere component of the reorganization energy λ_{os} is less variable among the ions due to the similarities in ion sizes.

Across an isostructural series, where any particular metal

Table 5. Comparison of Fe^{2+} oxidation $\log k_{12}$'s ($M^{-1} s^{-1}$) calculated in this study for the outer-sphere pathway with rate constants from experiments reported elsewhere.

	This study $\mu = 0.0$	This study $\mu = 0.7$	King (1998) $\mu = 0$	Wehrli (1990) ^{a,e} $\mu = ?^d$	Millero (1985) ^{b,e} $\mu = 0$	Lowson (1982) ^{c,e} $\mu = 3$
$Fe(OH_2)_6^{2+/3+}$	-5.8	-6.6	-6.04	-5.7	—	-6.2
$Fe(OH_2)_5(OH)^{1+/2+}$	-1.7	-2.2	0.84	0.8	0.8	—
$Fe(OH_2)_4(OH)_2^{0/1+}$	2.2	2.0	5.94	6.3	6.2	—

^a Wehrli fit the rate law of Millero (1985) to the combined data of Singer and Stumm (1970) and Millero et al. (1987).

^b Calculated from pseudo-first order rate constants in Millero (1985) using the Henry's law constant for O_2 at $25^\circ C = 1.26 \times 10^{-3} M atm^{-1}$ (see Wehrli, 1990).

^c The average of values from refs 219, 223, 231 reported in Table VII of Lowson (1982) (temperature = $30^\circ C$, media = $1 M H_2SO_4$).

^d Estimated to be $\sim 0.01 M$ based on the Singer and Stumm (1970) work in moderately dilute solutions ($\sim 0.01 M$) and assuming the dilute solution family of data ($0.009 M NaHCO_3$) was used from Millero et al. (1987).

^e These authors reported rates for the disappearance of Fe^{2+} whereas this study and King (1998) report reduction rates for O_2 , which should differ by a factor of 4 assuming the Haber-Weiss mechanism (see Eqn. 1-4 in text). Therefore, here the Wehrli (1990), Millero (1985), and Lowson (1982) rates are divided by 4 for comparison with the results of this study.

complex undergoes hydrolysis, modifications to the thermodynamic driving force for the electron transfer step ΔG° come in two forms. The creation of hydroxyl ligands in the complex modifies the reducing power of the metal atom. As a distinctly separate outcome, hydrolysis also modifies the driving force by altering the electrostatic work terms describing the interactions occurring, in this case, between the net charges on the product species. This is so because the work terms are used to adjust the overall thermodynamic driving force ΔG° to that occurring in the electron transfer step in the encounter complex. These effects combine to have a large influence on the rate of the oxidation cross-reaction.

An inner-sphere pathway for the self-exchange reactions and oxidation by O_2 of Mn^{2+} and Cr^{2+} ions has been supported indirectly in this study by exposition of the outer-sphere rates and comparison with experiments. Likewise, an outer-sphere pathway has been supported for the similar set of reactions involving the V, Fe, and Co ions. An assessment of the self-exchange reaction for the $O_2^{0/1-}$ couple has led to predicted rates in excellent agreement with direct measurements. Predicted rates of oxidation for the hexaquo Fe ion are also in remarkable agreement with experiment, while the predicted rates for the outer-sphere oxidation of its hydrolysis products are ~ 2 to 3 ($x = 1$) and ~ 4 ($x = 2$) orders of magnitude slower than the observed rates, suggesting an inner-sphere pathway is appropriate to explain the relatively fast rates observed for the hydrolyzed species. (Table 5)

Acknowledgments—We are grateful for the comments of T. W. Swaddle and an anonymous reviewer, which significantly improved the manuscript. Sponsored by the U.S. Department of Energy, Office of Basic Energy Sciences, Engineering and Geosciences Division. Pacific Northwest National Laboratory is operated for the DOE by Battelle Memorial Institute under Contract DE-AC06-76RLO 1830.

Associate editor: W. H. Casey

REFERENCES

- Allredge A. L. and Cohen Y. (1987) Can microscale chemical patches persist in the sea - Microelectrode study of marine snow, fecal pellets. *Science* **235**, 689–691.
- Anderson A. and Bonner N. A. (1954) The exchange reaction between chromous and chromic ions in perchloric acid solution. *J. Am. Chem. Soc.* **76**, 3826–3830.
- Bakac A. and Espenson J. H. (1993) Chromium complexes derived from molecular oxygen. *Accounts Chem. Res.* **26**, 519–523.
- Bakac A., Scott S. L., Espenson J. H., and Rodgers K. R. (1995) Interaction of chromium(II) complexes with molecular oxygen - Spectroscopic and kinetic evidence for η^1 -superoxo complex formation. *J. Am. Chem. Soc.* **117**, 6483–6488.
- Becke A. D. (1993) A new mixing of Hartree-Fock and local density functional theories. *J. Chem. Phys.* **98**, 1372–1377.
- Benner S. G., Gould W. D., and Blowes D. W. (2000) Microbial populations associated with the generation and treatment of acid mine drainage. *Chem. Geol.* **169**, 435–448.
- Bricker O. (1965) Some stability relations in the system Mn-O₂-H₂O at 25°C and 1 atmosphere total pressure. *Am. Mineral.* **50**, 1296–1354.
- Brunschwig B. S., Logan J., Newton M. D., and Sutin N. (1980) A semi-classical treatment of electron exchange reactions - Application to the hexaquoiron(II)-hexaquoiron(III) system. *J. Am. Chem. Soc.* **102**, 5798–5809.
- Brunschwig B. S., Creutz C., Macartney D. H., Sham T. K., and Sutin N. (1982) The role of inner-sphere configuration changes in electron exchange reactions of metal complexes. *Faraday Discuss.* **74**, 113–127.
- Bu Y. X. and Liu C. B. (1999) O₂+O₂⁻ electron transfer reactivity in the quartet state from ab initio calculation including electron correlation. *J. Mol. Struct-Theochem.* **490**, 7–20.
- Bu Y. X., Wang Y. X., Xu F. Q., and Deng C. H. (1998) Direct evaluation of the electron transfer integral for self-exchange reactions in solution. *J. Mol. Struct-Theochem.* **453**, 43–48.
- Bu Y. X., Sun H. T., and Niu H. B. (1999) Electron transfer reactivity of O₂+O₂⁻ system in low-spin coupling: Ab initio study at electron correlation level. *J. Comp. Chem.* **20**, 989–998.
- Clark T., Chandrasekhar J., Spitznagel G. W., and Schleyer P. V. (1983) Efficient diffuse function augmented basis sets for anion calculations. III. The 3-21+G basis set for 1st-row elements, Li-F. *J. Comp. Chem.* **4**, 294–301.
- Creutz C. and Sutin N. (1986) General reactivity patterns in electron transfer. In *Electron-Transfer and Electrochemical Reactions; Photochemical and Other Energized Reactions*, Vol. 15 (ed. J. J. Zuckermann), pp. 47–68 VCH, Deerfield Beach, Florida.
- Diebler H. and Sutin N. (1964) The kinetics of some oxidation-reduction reactions involving manganese (III). *J. Phys. Chem.* **68**, 174–180.
- Diem D. and Stumm W. (1984) Is dissolved Mn²⁺ being oxidized by O₂ in absence of Mn-bacteria or surface catalysts? *Geochim. Cosmochim. Acta* **48**, 1571–1573.
- Emerson S., Kalthorn S., Jacobs L., Tebo B. M., Nealson K. H., and Rosson R. A. (1982) Environmental oxidation rate of manganese(II) - Bacterial catalysis. *Geochim. Cosmochim. Acta* **46**, 1073–1079.
- Fallab S. (1967) Reactions with molecular oxygen. *Angew. Chem. Int. Ed.* **6**, 496–507.
- Frisch M. J., Trucks G. W., Schlegel H. B., Scuseria J. A., Robb M. A., Cheeseman J. R., Zakrzewski V. G., Montgomery J. A., Stratmann R. E., Burant J. C., Dapprich S., Millam J. M., Daniels A. D., Kudin K. N., Strain M. C., Farkas O., Tomasi J., Barone V., Cossi M., Cammi R., Mennucci B., Pomelli C., Adamo C., Clifford S., Ochterski J., Petersson G. A., Ayala P. Y., Cui Q., Morokuma K., Malick D. K., Rabuck A. D., Raghavachari K., Foresman J. B., Cioslowski J., Ortiz J. V., Stefanov B. B., Liu G., Liashenko A., Piskorz P., Komaromi I., Gomperts R., Martin R. L., Fox D. J., Keith T., Al-Laham M. A., Peng C. Y., Nanayakkara A., Gonzalez C., Challacombe M., Gill P. M. W., Johnson B., Chen W., Wong M. W., Andres J. L., Gonzalez C., Head-Gordon M., Replogle E. S., Pople J. A. (1998) Gaussian98. (Revision A.4). Gaussian, Inc.
- Gardiner W. C. Jr. (1969) *Rates and Mechanisms of Chemical Reactions*. W. A. Benjamin.
- German E. D., Kuznetsov A. M., Efremenko I., and Sheintuch M. (1999) Theory of the self-exchange electron transfer in the dioxygen/superoxide system in water. *J. Phys. Chem. A* **103**, 10699–10707.
- Giovanoli R. (1980) On natural and synthetic manganese nodules. In *Geology and Geochemistry of Manganese*, Vol. 1 (ed. I. M. Varentsov and G. Grasselly). E. Schweizerbart'sche Verlagsbuchhandlung (Nagele u. Obermiller).
- Goddard W. A. and Olafson B. D. (1975) Ozone model for bonding of an O₂ to heme in oxyhemoglobin. *P. Natl. Acad. Sci.* **72**, 2335–2339.
- Haber F. and Weiss J. P. (1934) *Roy. Soc. Lond. A* **A147**, 332.
- Habib H. S. and Hunt J. P. (1966) Electron transfer reactions between aqueous cobaltous and cobaltic ions. *J. Am. Chem. Soc.* **88**, 1668–1671.
- Hay P. J. (1977) Gaussian basis sets for molecular calculations. The representation of 3d orbitals in transition-metal atoms. *J. Chem. Phys.* **66**, 4377.
- Hem J. D. (1963) Chemical equilibria and rates of manganese oxidation. *U. S. Geol. Soc. Wat. Suppl.* **1667-A**, A1–A64.
- Jolley W. H., Stranks D. R., and Swaddle T. W. (1990) Pressure effect on the kinetics of the hexaquoiron(II/III) self-exchange reaction in aqueous perchloric acid. *Inorg. Chem.* **29**, 1948–1951.
- Keating E. H. and Bahr J. M. (1998) Reactive transport modeling of redox geochemistry: Approaches to chemical disequilibrium and reaction rate estimation at a site in northern Wisconsin. *Water Resour. Res.* **34**, 3573–3584.
- King D. W. (1998) Role of carbonate speciation on the oxidation rate of Fe(II) in aquatic systems. *Env. Sci. Tech.* **32**, 2997–3003.
- King D. W., Lounsbury H. A., and Millero F. J. (1995) Rates and mechanism of Fe(II) oxidation at nanomolar total iron concentrations. *Environ. Sci. Technol.* **29**, 818–824.

- Klimkans A. and Larsson S. (1994) Reorganization energies in benzene, naphthalene, and anthracene. *Chem. Phys.* **189**, 25–31.
- Krishnamurty K. V. and Wahl A. C. (1958) Kinetics of the vanadium(II)-vanadium(III) isotopic exchange reaction. *J. Am. Chem. Soc.* **80**, 5921–5924.
- Lappin G. (1994) *Redox Mechanisms in Inorganic Chemistry*. Ellis Horwood.
- Lasaga A. C. (1998) *Kinetic Theory in the Earth Sciences*. Princeton University Press.
- Lee C. T., Yang W. T., and Parr R. G. (1988) Development of the Colle-Salvetti correlation energy formula into a functional of the electron density. *Phys. Rev. B* **37**, 785–789.
- Li J., Fisher C. L., Chen J. L., Bashford D., and Noodleman L. (1996) Calculation of redox potentials and pK_a values of hydrated transition metal cations by a combined density functional and continuum dielectric theory. *Inorg. Chem.* **35**, 4694–4702.
- Lide D. R. (1990) *Handbook of Chemistry and Physics*. CRC Press.
- Lind J., Shen X., Merenyi G., and Jonsson B. O. (1989) Determination of the rate constant of self-exchange of the O_2/O_2^- couple in water by O^{18}/O^{16} isotope marking. *J. Am. Chem. Soc.* **111**, 7654–7655.
- Logan J. and Newton M. D. (1983) Ab initio study of electronic coupling in the aqueous $Fe^{2+}-Fe^{3+}$ electron exchange process. *J. Chem. Phys.* **78**, 4086–4091.
- Lowson R. T. (1982) Aqueous oxidation by molecular oxygen. *Chem. Rev.* **82**, 461–497.
- Luther G. W. III (1990) The frontier-molecular orbital theory approach in geochemical processes. In *Aquatic Chemical Kinetics* (ed. W. Stumm) 173–198. John Wiley & Sons.
- Macartney D. H. and Sutin N. (1985) Kinetics of the oxidation of metal complexes by manganese(III) aquo ions in acidic perchlorate media - The $Mn(H_2O)_6^{2+}-Mn(H_2O)_6^{3+}$ electron exchange rate constant. *Inorg. Chem.* **24**, 3403–3409.
- Marcus R. A. (1956) On the theory of oxidation-reduction reactions involving electron transfer. *J. Chem. Phys.* **24**, 966–978.
- Marcus R. A. and Sutin N. (1985) Electron transfers in chemistry and biology. *Biochim. Biophys. Acta* **811**, 265–322.
- Martin R. L., Hay P. J., and Pratt L. R. (1998) Hydrolysis of ferric ion in water and conformational equilibrium. *J. Phys. Chem. A* **102**, 3565–3573.
- McGuire J. T., Smith E. W., Long D. T., Hyndman D. W., Haack S. K., Klug M. J., and Velbel M. A. (2000) Temporal variations in parameters reflecting terminal electron accepting processes in an aquifer contaminated with waste fuel and chlorinated solvents. *Chem. Geol.* **169**, 471–485.
- Miertus S. and Tomasi J. (1982) Approximate evaluations of the electrostatic free energy and internal energy changes in solution processes. *Chem. Phys.* **65**, 239–245.
- Miertus S., Scrocco E., and Tomasi J. (1981) Electrostatic interaction of a solute with a continuum - A direct utilization of ab initio molecular potentials for the prevision of solvent effects. *Chem. Phys.* **55**, 117–129.
- Millero F. J. (1985) The effect of ionic interactions on the oxidation of metals in natural waters. *Geochim. Cosmochim. Acta* **49**, 547–553.
- Millero F. J. (1989) Effect of ionic interactions on the oxidation of Fe(II) and Cu(I) in natural waters. *Mar. Chem.* **28**, 1–18.
- Millero F. J. and Izaguirre M. (1989) Effect of ionic strength and ionic interactions on the oxidation of Fe(II). *J. Sol. Chem.* **18**, 585–599.
- Millero F. J., Sotolongo S., and Izaguirre M. (1987) The oxidation kinetics of Fe(II) in seawater. *Geochim. Cosmochim. Acta* **51**, 793–801.
- Morgan J. J. (1967) Chemical equilibria and kinetic properties of manganese in natural waters. In *Principles and Applications of Water Chemistry* (eds. S. Faust and J. Hunter), pp. 561–624. John Wiley & Sons.
- Nordin J. P., Sullivan D. J., Phillips B. L., and Casey W. H. (1998) An O^{17} -NMR study of the exchange of water on $AlOH(H_2O)_5^{2+}$ (aq). *Inorg. Chem.* **37**, 4760–4763.
- Ohta K. and Morokuma K. (1987) An ab initio MO study on electron transfer in gas phase hydrated clusters: $O_2^-(H_2O)_n + O_2 \rightarrow O_2 + O_2^-(H_2O)_n$ ($n = 0, 1, \text{ and } 2$). *J. Phys. Chem.* **91**, 401–406.
- Olafson B. D. and Goddard W. A. (1977) Molecular description of dioxygen bonding in hemoglobin. *P. Natl. Acad. Sci.* **74**, 1315–1319.
- Ricca A. and Bauschlicher C. W. (1994) Successive binding energies of $Fe(Co)^{5+}$. *J. Phys. Chem.* **98**, 12899–12903.
- Richens D. T. (1997) *The Chemistry of Aqua Ions*. Wiley.
- Rosso K. M. and Rustad J. R. (2000) Ab initio calculation of homogeneous outer sphere electron transfer rates: Application to $M(OH)_6^{3+/2+}$ redox couples. *J. Phys. Chem. A* **104**, 6718–6725.
- Rush J. D. and Bielski B. H. J. (1985) Kinetics and mechanism of oxidation of vanadium (II) by molecular oxygen and hydrogen peroxide. *Inorg. Chem.* **24**, 4282–4285.
- Russo T. V., Martin R. L., and Hay P. J. (1995) Application of gradient corrected density functional theory to the structures and thermochemistries of ScF_3 , TiF_4 , VF_5 , and CrF_6 . *J. Chem. Phys.* **102**, 8023–8028.
- Rustad J. R., Dixon D. A., Rosso K. M., and Felmy A. R. (1999) Trivalent ion hydrolysis reactions: A linear free energy relationship based on density functional electronic structure calculations. *J. Am. Chem. Soc.* **121**, 3234–3235.
- Scherlis D. A. and Estrin D. A. (2002) Structure and spin-state energetics of an iron porphyrin model: An assessment of theoretical methods. *Int. J. Quantum Chem.* **87**, 158–166.
- Sellers R. M. and Simic M. G. (1976) Pulse radiolysis study of the reactions of some reduced metal ions with molecular oxygen in aqueous solution. *J. Am. Chem. Soc.* **98**, 6145–6150.
- Silverman J. and Dodson R. W. (1952) The exchange reaction between the two oxidation states of iron in acid solution. *J. Phys. Chem.* **56**, 846–852.
- Singer P. C. and Stumm W. (1970) Acidic mine drainage: The rate-determining step. *Science* **167**, 1121–1123.
- Smith R. M. and Martell A. E. (1979) *Critical Stability Constants*. Plenum Press.
- Stanbury D. M., Haas O., and Taube H. (1980) Reduction of Oxygen by Ruthenium(II) Amines. *Inorg. Chem.* **19**, 518–524.
- Stumm W. and Morgan J. J. (1996) *Aquatic Chemistry*. John Wiley & Sons.
- Sung W. and Morgan J. J. (1981) Oxidative removal of Mn(II) from solution catalyzed by the γ - $FeOOH$ (lepidocrocite) surface. *Geochim. Cosmochim. Acta* **45**, 2377–2383.
- Sutin N. (1986) Theory of electron transfer reactions. In *Electron-Transfer and Electrochemical Reactions; Photochemical and Other Energized Reactions*, Vol. 15 (ed. J. J. Zuckermann), pp. 16–47 VCH. Dearfield Beach, Florida.
- Swinehart J. H. (1965) On the oxidation of vanadium(II) by oxygen and hydrogen peroxide. *Inorg. Chem.* **4**, 1069–1070.
- Tembe B. L., Friedman H. L., and Newton M. D. (1982) The theory of the $Fe^{2+}-Fe^{3+}$ electron exchange in water. *J. Chem. Phys.* **76**, 1490–1507.
- Wachters A. J. H. (1970) Gaussian basis set for molecular wavefunctions containing third-row atoms. *J. Chem. Phys.* **52**, 1033.
- Wagman D. D., Evans W. H., Parker V. B., Halow I., Bailey S. M., and Schumm R. H. (1968) Selected values of chemical thermodynamic properties. Tables for the first thirty-four elements in the standard order of arrangement. *United States National Bureau of Standards Technical Note* **270-3**, 1–264.
- Weaver M. J. and Lee E. L. (1980) Activation parameters for homogeneous outer-sphere electron transfer reactions. Comparisons between self-exchange and cross reactions using Marcus' theory. *Inorg. Chem.* **19**, 1936–1945.
- Wehrli B. (1990) Redox reactions of metal ions at mineral surfaces. In *Aquatic Chemical Kinetics* (ed. W. Stumm), pp. 311–336. John Wiley & Sons.
- Zahir K., Espenson J. H., and Bakac A. (1988) Reactions of polypyridylchromium(II) ions with oxygen - Determination of the self-exchange rate constant of O_2/O_2^- . *J. Am. Chem. Soc.* **110**, 5059–5063.